

## Analytical method for predicting the quasi-static buffeting response of transmission conductor under non-stationary winds

Dahai Wang<sup>1</sup>, Xinzhong Chen<sup>2</sup>

<sup>1</sup>Department of Civil Engineering

Wuhan University of Technology, Wuhan, 430070, China

<sup>2</sup>National Wind Institute, Department of Civil, Environmental and Construction Engineering

Texas Tech University, Lubbock, 79409, USA

### Abstract

Most failures of transmission towers are attributed to the actions of severe thunderstorm downbursts and tornadoes with non-stationary characteristics. This paper presents an analytical framework for predicting quasi-static buffeting response of a conductor when subjected to the non-stationary wind excitations. The analytical solutions of nonlinear time-varying mean response as well as influence functions around the static equilibrium are derived for arbitrary spatial and temporal variations of the mean wind speed. The time-varying standard derivation (STD) of response is directly calculated using the influence function and correlation function of wind fluctuations. The framework also permits calculation of probability distribution of extreme response and peak factor from the time-varying mean and STD of response. The efficiency and accuracy of the framework are demonstrated through comparison of response predictions from a nonlinear dynamic finite element (FE) analysis.

### Introduction

Many transmission tower failures worldwide are reported to be attributed to the actions of localized non-synoptic winds, such as thunderstorm downbursts and tornadoes [4,6,10]. The wind flow field created by a thunderstorm wind can vary significantly from the traditional atmospheric boundary layer wind flows in terms of its unique mean wind speed profile, rapid time-varying mean wind speed, and spatially strongly correlated wind fluctuations [2, 3]. A number of studies have examined the non-stationary wind load effects on transmission line structures using time-varying mean wind speed field generated by empirical models or computational fluid dynamics (CFD) simulations [1,11,12]. The wind load on the conductor is generally calculated from the wind fluctuation using quasi-steady theory. The system response is then calculated in the time domain using a finite element model (FEM) with consideration of structural geometric nonlinearity. Aboshosha [1] introduced a numerical iteration scheme using semi-closed and close-from solutions for predicting the nonlinear static conductor response under time-varying mean wind loads with arbitrary spatial distributions. Previous studies have shown that the resonant dynamic response of conductor can be neglected because of the effect of large aerodynamic damping [1,7,9].

This paper addresses analytical method for the dynamic buffeting response of a conductor under non-synoptic wind excitations. The wind speed and conductor response are characterized by deterministic time-varying mean and stochastic fluctuating components. The time-varying mean response is calculated by nonlinear static analysis with an analytical solution. The stochastic dynamic response is considered as quasi-static

(background) response whose time-varying STD is calculated from response influence function and correlation function of wind fluctuations. The peak factor and gust response factor are determined using mean upcrossing rate theory of non-stationary random process. The effectiveness and accuracy of the proposed analytical framework are verified through response time history analysis using nonlinear FEM.

### Modelling of transmission conductor and wind load

A horizontal transmission conductor hinged on both supports at the same elevation is considered. It is modelled as a uniform flat-sag suspended cable with a sag to span ratio of 1/30~1/50. The initial line position under its gravity  $mg$  and a longitudinal tension  $H_0$  is denoted as  $y_0(x)$ , which is a parabola with a sag  $d_0$  as shown in Fig.1:

$$y_0(x) = \frac{mg}{2H_0}x(L-x) \quad (1)$$

$$d_0 = \frac{mgL^2}{8H_0} \quad (2)$$

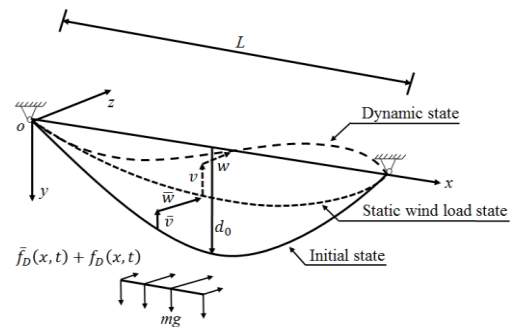


Fig. 1. Profile of the conductor under wind load

The mean wind speed is perpendicular to the initial conductor plan. The wind speed at the span-wise location  $x$ ,  $V_c(x,t)$ , is a sum of deterministic time-varying mean wind speed component  $\bar{V}(x,t)$  and random fluctuating component  $V(x,t)$  as

$$V_c(x,t) = \bar{V}(x,t) + V(x,t) \quad (3)$$

The mean and dynamic lateral (drag) wind forces per unit length of the conductor are calculated as follows based on quasi-steady theory:

$$\bar{f}_D(x,t) = \frac{1}{2} \rho DC_D \bar{V}^2(x,t) \quad (4)$$

$$f_D(x,t) = \rho DC_D \bar{V}(x,t)V(x,t) \quad (5)$$

where  $\rho$  is air density;  $C_D$  is the static drag coefficient; and  $D$  is diameter of the conductor. The dynamic deformations of the conductor in vertical (crosswind) and lateral (alongwind) directions,  $v_c(x, t)$  and  $w_c(x, t)$ , are expressed as sum of deterministic time-varying mean component,  $\bar{v}(x, t)$  and  $\bar{w}(x, t)$ , and stochastic dynamic component,  $v(x, t)$  and  $w(x, t)$ , as:

$$v_c(x, t) = \bar{v}(x, t) + v(x, t) \quad (6)$$

$$w_c(x, t) = \bar{w}(x, t) + w(x, t) \quad (7)$$

### Analyses of time-varying mean response and influence function

The nonlinear and coupled equations of motion of the conductor under both static wind load and weight are expressed as [5]:

$$\bar{H}(t) \frac{d^2(y_0(x) + \bar{v}(x, t))}{dx^2} = -mg \quad (8)$$

$$\bar{H}(t) \frac{d^2\bar{w}(x, t)}{dx^2} = -\bar{f}_D(x, t) \quad (9)$$

The compatibility condition of the conductor leads to

$$\begin{aligned} \frac{(\bar{H}(t) - H_0)L_e}{EA} &= \frac{mg}{H_0} \int_0^L \bar{v}(x, t) dx \\ &+ \frac{1}{2} \int_0^L \left( \frac{d\bar{v}(x, t)}{dx} \right)^2 dx \\ &+ \frac{1}{2} \int_0^L \left( \frac{d\bar{w}(x, t)}{dx} \right)^2 dx \end{aligned} \quad (10)$$

where  $E$  is Young's modulus;  $A$  is the cross sectional area of the conductor;  $L_e$  is a virtual length of the cable and  $L_e \approx L$ .

The solution of Eqs. (8) and (9) can be obtained readily by direct integrations considering the boundary conditions:

$$\bar{v}(x, t) = \frac{(H_0 - \bar{H}(t)) mg}{\bar{H}(t) 2H_0} (L - x) \quad (11)$$

$$\begin{aligned} \bar{w}(x, t) &= \frac{1}{\bar{H}(t)} \left( \frac{x}{L} \int_0^L \int_0^x (\bar{f}_D(x, t) dx) dx \right. \\ &\quad \left. - \int_0^x \int_0^x (\bar{f}_D(x, t) dx) dx \right) \end{aligned} \quad (12)$$

where the boundary conditions for  $\bar{w}(x, t)$  and  $\bar{v}(x, t)$  are  $\bar{w}(0, t) = \bar{w}(L, t) = \bar{v}(0, t) = \bar{v}(L, t) = 0$ . Substituting Eqs.(11) and (12) to Eq.(10) leads to the equation of  $\bar{H}(t)$ :

$$\bar{H}(t) - H_0 = \frac{EAL^2}{24} \left( \frac{q^2(t)}{\bar{H}^2(t)} - \frac{(mg)^2}{H_0^2} \right) \quad (13)$$

where  $q(t) = \sqrt{(mg)^2 + f_*^2(t)}$ ;  $f_*(t)$  is given as follows and can be considered as the equivalent uniform load

$$f_*^2(t) = \frac{12}{L^3} \int_0^L \left[ \int_0^L \bar{f}_D(x, t) \left(1 - \frac{x}{L}\right) dx - \int_0^x \bar{f}_D(x, t) dx \right]^2 dx \quad (14)$$

Obviously, when  $\bar{f}_D(x, t)$  follows a uniform distribution along the span, there will be  $\bar{f}_D(x, t) = \bar{f}_D(t) = f_*(t)$ .

The time-varying mean tension components in three directions at the ends of conductor are determined from equations of force equilibrium of the overall system as

$$\bar{T}_x(t) = \bar{H}(t); \quad \bar{T}_y = \frac{1}{2} mgL; \quad (15)$$

$$\bar{T}_z(t) = \int_0^L \bar{f}_D(x, t) \mu_{T_z}(x, t) dx$$

where  $\mu_{T_z}(x, t) = 1 - x/L$  is the influence function of  $T_z(t)$ .

On the static equilibrium under mean wind load  $\bar{f}_D(x, t)$ , based on the cable mechanics, the linear influence function of the additional longitudinal reaction, i.e.,  $\mu_{T_x}(x_1, t)$ , can be given as below

$$\begin{aligned} \mu_{T_x}(x_1, t) &= \frac{\int_0^{x_1} \bar{f}_D(x, t) x dx - \left(\frac{x_1}{L}\right) \int_0^L \bar{f}_D(x, t) x dx + x_1 \int_{x_1}^L \bar{f}_D(x, t) dx}{\left(\frac{\bar{H}^2 L}{EA} + \frac{m^2 g^2 L^3}{12 \bar{H}} + \int_0^L \bar{f}_D(x, t) \bar{w} dx\right)} \end{aligned} \quad (16)$$

For the vertical displacement at location  $x$ , i.e.,  $v(x, t)$ , we have:

$$\mu_v(x_1, t) = -\frac{y_0(x) + \bar{v}(x, t)}{\bar{H}(t)} \mu_{T_x}(x_1, t) \quad (17)$$

For the lateral displacement at location  $x$ , i.e.,  $w(x, t)$ , we have:

$$\begin{aligned} \mu_w(x_1, t) &= \begin{cases} \frac{1}{\bar{H}(t)} \left\{ \left(-\frac{x_1}{L}\right) x + x_1 - \mu_{T_x}(x_1, t) \bar{w}(x, t) \right\} & (0 < x_1 \leq x) \\ \frac{1}{\bar{H}(t)} \left\{ \left(1 - \frac{x_1}{L}\right) x - \mu_{T_x}(x_1, t) \bar{w}(x, t) \right\} & (x < x_1 \leq L) \end{cases} \end{aligned} \quad (18)$$

### Analysis of quasi-static dynamic response

The dynamic response is considered as quasi-static background response, and is determined directly from the influence function under the dynamic wind load as

$$r(t) = \int_0^L \mu(x, t) f_D(x, t) dx \quad (19)$$

where  $\mu(x, t)$  is the influence function, denoting the response of  $r$  due to unit static load at spanwise location  $x$  in lateral direction. The dependence of influence function on time is because that the static equilibrium is time-varying.

The variance of the dynamic response is then calculated by

$$\begin{aligned} \sigma_r^2(t) &= (\rho DC_D)^2 \\ &\int_0^L \int_0^L \bar{V}(x_1, t) \bar{V}(x_2, t) \mu(x_1, t) \mu(x_2, t) R_V(x_1, x_2, t) dx_1 dx_2 \end{aligned} \quad (20)$$

$$\begin{aligned} R_V(x_1, x_2, t) &= \int_{-\infty}^{\infty} g_V(x_1, \omega, t) g_V^*(x_2, \omega, t) S_{V_0}(x_1, x_2, \omega) d\omega \end{aligned} \quad (21)$$

where  $g_V(x, \omega, t)$  is modulation function for wind fluctuation and  $g_V^*(x, -\omega, t)$ ;  $S_{V_0}(x_1, x_2, \omega)$  are the cross power spectral density (PSD) - function of the underlying stationary process of wind fluctuations;

The distribution of extreme value of  $r(t)$  within a time duration of  $T$ , i.e.,  $r_{\max} = \max[r(t), 0 \leq t \leq T]$ , is calculated through

mean upcrossing rate analysis. The response  $r(t)$  is treated as an evolutionary Gaussian process. The cumulative distribution function of the extreme response is calculated as follows under the assumption of Poisson crossings [8]:

$$F_{\max}(r) = \exp \left[ - \int_0^T \nu(r, t) dt \right] \quad (22)$$

$$\nu(r, t) = \frac{1}{2\pi} \frac{\sigma_{\dot{r}}(t)}{\sigma_r(t)} \exp \left\{ - \frac{[r - \bar{r}(t)]^2}{2\sigma_r^2(t)} \right\} \quad (23)$$

where  $\nu(r, t)$  is mean single barrier crossing rate at level  $r$ ;  $\sigma_{\dot{r}}(t)$  is the STD of  $\dot{r}(t)$ , which can be calculated using Eq. (20) and (21), but  $S_{V_0}(x_1, x_2, \omega)$  is replaced by  $\omega^2 S_{V_0}(x_1, x_2, \omega)$ ; and  $\bar{r}(t)$  is the time-varying mean of  $r(t)$ .

The mean extreme  $r_{\mu\max}$  is subsequently determined as 57%-fractile value as the extreme value distribution approaches to Gumbel distribution at high levels of extreme. The peak factor and gust response factor (GRF) are defined as  $g = (r_{\mu\max} - \bar{r}_{\max})/\sigma_{r\max}$  and  $G = r_{\mu\max}/\bar{r}_{\max}$ , where  $\bar{r}_{\max}$  and  $\sigma_{r\max}$  are maximum values of  $\bar{r}(t)$  and  $\sigma_r(t)$  over the time duration  $T$ . In the case of stationary wind excitation, the peak factor reduces to the closed-form expression by Davenport (1964).

### Validation of the analysis approach

#### Characteristics of the conductor and wind field

A 500-kV prototype single conductor is considered, which has the following parameters: span length  $L=400$  m, sag ratio  $d_0/L = 1/30$ , the reference height, i.e.,  $2/3d_0$  below the support level,  $z = 61$  m, uniform mass  $m = 2.39$  kg/m, diameter  $D = 0.036$  m,  $EA = 48.8 \times 10^3$  kN, initial tension  $H_0 = 35.20$  kN, and the Irvine number  $\lambda^2 = 98.6$ . The conductor is subjected to the lateral wind excitation in the direction perpendicular to the conductor plane. The drag force coefficient  $C_D = 1.0$ . The time-varying mean wind speed and random wind fluctuation are assumed to have the following variations

$$\bar{V}(x, t) = \bar{V}_{\max} \bar{V}_0(x) \bar{d}(t) \quad (24)$$

$$V(x, t) = V_0(x, t) V_1(x) d(t) \quad (25)$$

where  $\bar{V}_{\max}$  is maximum mean wind speed;  $V_0(x, t)$  is the underlying zero-mean stationary random process;  $\bar{V}_0(x)$  and  $V_1(x)$  are spanwise variation of mean wind speed and spanwise modulation function of wind fluctuation with their maximum values of unity;  $\bar{d}(t)$  and  $d(t)$  are the time-varying modulation functions for the mean and fluctuating wind speed. Here, the modulation function for the nonstationary wind fluctuation is  $g_V(x, \omega, t) = V_1(x) d(t)$ . In this example study, it is assumed that

$$\bar{V}_0(x) = V_1(x) = \left( 1 - \frac{x}{L} \right) \quad (26)$$

$$\bar{d}(t) = d(t) = \exp[-(t - t_0)^2/2D_t^2] \quad (27)$$

where  $t_0$  is the time instant at which  $\bar{d}(t)=d(t)$  reach their maximum values; and  $D_t$  is wind storm duration parameter. The power spectral character of the underlying stationary process  $V_0(x, t)$  is given by Kaimal spectrum with the coherence function given by Davenport's exponential function model, in which the decay factor  $C_\gamma=16$ . In this example study,  $\bar{V}_{\max} = 40$  m/s,  $D_t = 120$  s, and the STD of wind fluctuation is  $\sigma_{V_0}=4.42$  m/s.

### Comparison of time-varying mean response

The static response under time-varying mean wind load is calculated using a nonlinear FEM and is compared with the prediction from the analytical approach. The distorted yawing profile of the conductor shows a clear nonlinear deflection of the conductor in Fig.2. The profile does not remain in a inclined plane, which is different from the case with uniformly distributed loading [13]. The time variations of lateral and longitudinal reactions are shown in Fig.3. It is observed that the predictions of time-varying mean from FEM and analytical approach are very agreeable, which illustrates the accuracy of the analytical approach for calculation of time-varying mean response.

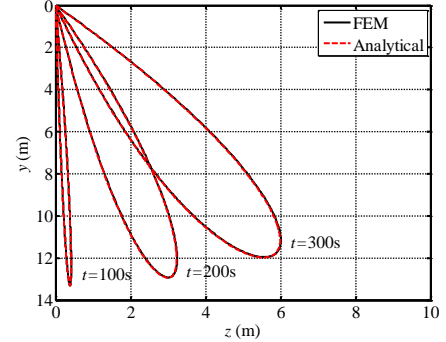


Fig. 2. The yawing profile of conductor under time-varying mean wind

### Comparison of dynamic response

The dynamic response calculated from both nonlinear FEM and analytical approach are also compared. In the FEM approach, the geometric nonlinearity of the conductor is also considered. The time histories of wind fluctuations are generated by using spectral representation method for given target spectral characteristics. The equations of motion are solved by using Newmark's step-by-step integration method.

It has been confirmed that the response time history determined from nonlinear FEM approach is almost identical to that directly from the analytical influence function under the same wind fluctuation input. Fig.4 show the comparison of time-varying STD determined from 100 response time history simulations with that from closed-form analytical estimation. It is evident that the closed-form solution gives accurate estimation of time-varying STD of response.

Table 1 Comparison of responses between simulation and close-form (kN)

	Lateral reaction				Longitudinal reaction			
	$\bar{r}_{\max}$	$\sigma_{r\max}$	$g$	$G$	$\bar{r}_{\max}$	$\sigma_{r\max}$	$g$	$G$
Simulation	3.7	0.70	1.3	1.2	39	1.3	1.2	1.0
Closed-form		0.63	1.7	1.2		1.2	1.6	1.0

The comparison of maximum values of time-varying mean and STD,  $\bar{r}_{\max}$  and  $\sigma_{r\max}$ , as well as the peak factor,  $g$ , and GRF,  $G$ , of lateral and longitudinal reactions are summarized in Table 1. In the analytical framework, mean maximum response is calculated using the upcrossing rate theory of nonstationary Gaussian response process. The results demonstrate that the analytical framework provides accurate estimation of extreme response.

A comprehensive parameter study regarding the influence of spatial and temporal variations of wind characteristics are

investigated using the analytical framework with closed-form solutions of response statistics. The results provide new insights on the response characteristics of conductor under various nonstationary wind excitations.

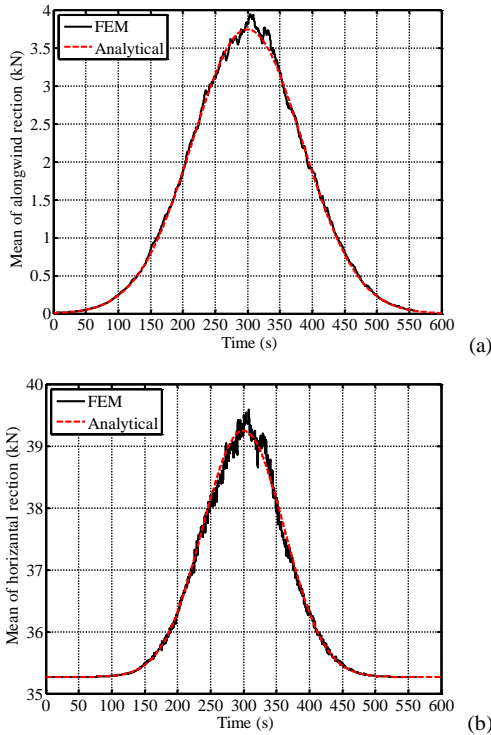


Fig. 3. Comparison of time-varying mean reaction response: (a) Lateral, (b) Longitudinal

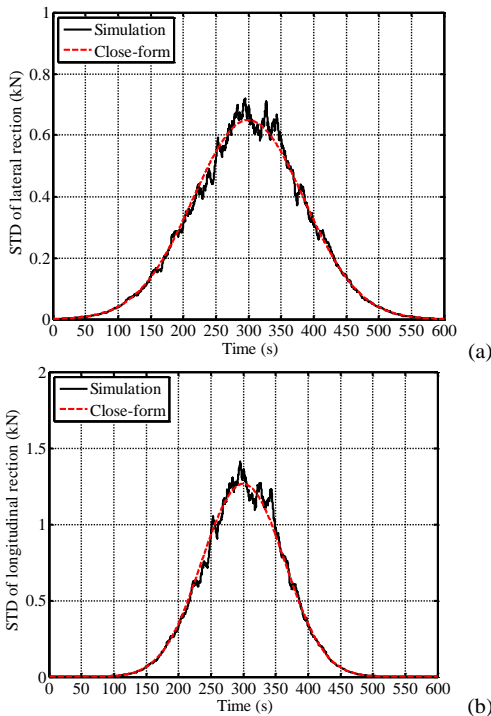


Fig. 4 Comparison of time-varying STD of reaction response: (a) Lateral, (b) Longitudinal

### Conclusions

An analytical framework was presented for estimation buffeting response of transmission conductor under non-stationary wind

excitations. It provided analytical solutions of time-varying mean, STD and extreme distribution of response. The efficiency and accuracy of the framework were demonstrated through comparison of response predictions from a nonlinear FEM analysis.

The peak factor and gust response factor of response under non-stationary wind excitation are much lower than those under stationary wind with constant wind speed due to lack of built-up time of dynamic response. The spatial variations of mean wind speed and wind characteristics have significant influence on response.

### Acknowledgments

This work is supported in part by National Natural Science Foundation of China (Grant No. 51478373 and 51478401). This support is greatly acknowledged.

### References

- [1] Aboshosha, H. and El Damatty, A., Engineering method for estimating the reactions of transmission line conductors under downburst winds, *Engineering Structures*, **99**, 2015, 272-284.
- [2] Fujita, T.T., Downbursts: meteorological features and wind field characteristics. *Journal of Wind Engineering and Industrial Aerodynamics*, **36**, 1990, 75-86.
- [3] Hangan, H., Roberts, D., Xu, Z., Kim, J., Downburst simulation: experimental and numerical challenges, in: *Proceedings of the 11th International Conference on Wind Engineering, Electronic Version*, Lubbock, TX, 2003.
- [4] Holmes, J.D., Hangan, H.M., Schroeder, J.L., Letchford, C.W. and Orwig, K.D. A forensic study of the Lubbock-Reese downdraft of 2002", *Wind Struct.*, **11**(2), 2008, 137-152.
- [5] Irvine H. M., *Cable Structures*. Cambridge (MA, USA): MIT Press, 1981.
- [6] Li, C.Q., A stochastic model of severe thunderstorms for transmission line design., *Probabilistic Engineering Mechanics*, **15**(4), 2000, 359-364.
- [7] Loredou-Souza, A.M. and Davenport, A.G., The effects of high winds on conductor. *Journal of Wind Engineering and Industrial Aerodynamics*, **74**, 1998, 987-994.
- [8] Lutes, Loren D., and Shahram S.. *Random vibrations: analysis of structural and mechanical systems*, Butterworth-Heinemann, 2004.
- [9] Matheson, M.J. and Holmes, J.D., Simulation of the dynamic response of conductor in strong winds. *Engineering Structures*, **3**(2), 1981, 105-110.
- [10] Oliver, S.E., Moriarty, W.W. and Holmes, J.D., A risk model for design of transmission line systems against thunderstorm downburst winds. *Engineering Structures*, **22**(9), 2000, 1173-1179.
- [11] Savory, E., Parke, G.A., Zeinoddini, M., Toy, N. and Disney, P., 2001. Modelling of tornado and microburst-induced wind loading and failure of a lattice transmission tower. *Engineering Structures*, **23**(4), pp.365-375.
- [12] Shehata, A.Y., El Damatty, A.A. and Savory, E., Finite element modeling of transmission line under downburst wind loading. *Finite Elements in Analysis and Design*, **42**(1), 2005, 71-89.
- [13] Wang, D., Chen, X., Li, J., Prediction of wind-induced buffeting response of overhead conductor: Comparison of linear and nonlinear analysis approaches, *Journal of Wind Engineering and Industrial Aerodynamics*, **167**, 2017, 23-40